Optica Applicata, Vol. LIII, No. 1, 2023
DOI: 10.37190/oa230107

Designing ultra-fast all-optical full-subtractor using the photonic crystal structure

FOROGH PAKRAI[1], MOHAMMAD SOROOSH[2,*], JABBAR GANJI[1]

[1]Department of Electrical Engineering, Mahshahr Branch, Islamic Azad University, Mahshahr, Iran

[2]Department of Electrical Engineering, Shahid Chamran University of Ahvaz, Ahvaz, Iran

[*]Corresponding author: m.soroosh@scu.ac.ir

In this paper, a photonic crystal-based structure for an all-optical full-subtractor has been proposed. The structure includes six nonlinear resonant rings to transmit the incoming optical waves toward the output ports. Using the different radii for nonlinear rods made the possibility of the dropping operation for different amounts of optical intensities. The nonlinear rods are made of a doped-glass with an optical Kerr coefficient of 10^{-15} m^2/W. To calculate the components of the optical waves throughout the structure, the finite-difference time-domain method has been used. The simulation results prove the correct functionality of the proposed structure. Besides, the maximum rise time of the device is equal to 2 ps. The contrast ratio and the area of the structure are around 8.08 dB and 2790 μm^2, respectively.

Keywords: full subtractor, nonlinear ring resonator, optical Kerr effect, photonic crystal.

1. Introduction

Due to high demands for high-speed processing and wide-bandwidth links, it is inevitable to find a better substitute for electronic-based communications and processing systems. Optical communications and optical processing are excellent ways that have been suggested. An optical system can work at the optimum speed when all of its building blocks be optical and no electronic device be used inside the system.

One of the fundamental structures that can be used for designing various types of optical devices is photonic crystal (PCs) [1]. One of the interesting capabilities of PCs is the switching threshold capability for resonant rings [2,3]. Based on this issue, different kinds of optical devices such as logic gates [4–9], decoders [2,10–13], encoders [14–17], adders [18–24], comparators [25–27], data converters [28–32], flip-flops [33,34], and multiplexers [35] have been designed.

Subtractors are crucial for implementing all-optical calculation systems. Therefore, different structures have been proposed for designing these PC-based devices [36–40]. PARANDIN *et al*. [36] proposed a PC-based structure to realize an optical half-subtractor.

They used the cross-connected waveguides including four rods at the center. Although the subtraction operation was obtained, the amount of the optical power at an input port was 1.5 times of one at another port. They improved the structure and obtained a rise time of 0.8 ps [37]. Using three nonlinear resonant rings, MORADI [38] succeeded in designing a structure for an optical half-subtractor. He used equal power at input ports, however the rise time was increased to 3 ps. An optical half-subtractor was proposed by ASKARIAN *et al*. [39], which used two nonlinear resonant rings and beam interference mechanisms for implementing the subtraction operation. They also reported the rise time of 1 ps. They proposed a linear structure for realizing an optical half-subtractor, which worked based on optical beam interference and phase shift keying technique [40]. The rise time of this structure was equal to 2 ps. Then, he designed another structure for the half-subtractor using nonlinear rings and succeeded in improving the rise time to 0.8 ps [41]. MIRALI *et al*. [42] presented a half-subtractor using two nonlinear rings and wave splitters. The rise time of the device was equal to 1.4 ps. NAMDARI *et al*. [43] realized an optical half-subtractor including nonlinear cavities to drop the optical waves towards the output ports. The rise time of the structure was around 1.5 ps. Recently, FANG *et al*. [44] have proposed a new structure based on a control port for designing a half-subtractor/half-adder. They reported a rise time of 1.5 ps. KHAJEHEIAN *et al*. [45] have recently designed a full-subtractor based on nonlinear rings. They calculated a value of 2.2 ps for the total rise and delay times, and the power consumption increased via an optical bias.

In this paper, we are going to design and propose a new all-optical full-subtractor. The proposed structure is realized using six nonlinear resonant rings. The rings couple the optical waves from a waveguide into another one if the amount of optical intensity is more than the switching threshold. The maximum rise time of the designed structure is around 2 ps and the contrast ratio is equal to 8.08 dB. In comparison to Ref. [45], the designed structure is faster. Also, the structure needs no optical bias to approach the correct operation so the power consumption does not increase.

The rest of the paper was organized as follows: in Section 2, we present the design procedure of the structure, the simulation results will be discussed in Section 3 and the conclusion comes in Section 4.

2. The proposed full-subtractor

The fundamental structure used for designing the optical full-subtractor includes a two -dimensional square lattice of silicon rods in the form of 77 rows and 91 columns. The refractive index and the radius of rods are 3.46 and 126 nm, respectively. Also, the lattice constant of the structure (a) is equal to 631 nm. The simulation results show that the mentioned lattice includes two photonic bandgaps (PBGs) in the ranges of 0.28–0.42 and 0.72–0.74. Concerning $a = 631$ nm, the larger bandgap is between 1502 and 2254 nm which covers C and L bands. In this research, the wavelength of 1550 nm is used for incoming optical signals so they are allowed to transmit through the optical waveguides.

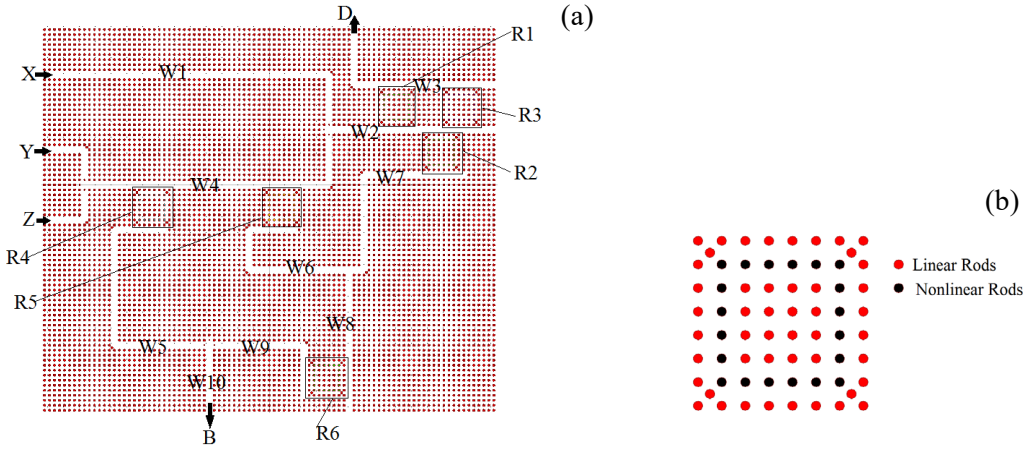

Fig. 1. (a) The proposed structure, and (b) the used resonant ring.

For designing the structure, six nonlinear resonant rings connect X, Y, and Z input ports to B and D output ports. Corresponding to the different working states, these rings guide the optical waves toward the desired paths. They are labeled as R1, R2, R3, R4, R5, and R6 as shown in Fig. 1(a). The resonators are created by adding some nonlinear rods made of a doped glass inside them (Fig. 1(b)).

When an optical power illuminates a nonlinear rod, the refractive index of the rod (n) changes due to the optical Kerr effect. The Kerr effect is known as $n = n_0 + n_1 I$ where n_0 and n_1 are the initial refractive index and Kerr coefficient, respectively. In other words, the refractive index corresponds to an applied optical intensity (I). By using the nonlinear rods in a photonic crystal ring resonator, the effective refractive index of the ring depends on the incoming optical intensity. So, the coupling efficiency changes for different amounts of optical intensity. Concerning all working states of the device, different powers reach the rings, and the coupling efficiency changes. This feature makes a possibility to guide the incoming waves toward the correct output ports, and design the photonic crystal-based devices.

The linear refractive index and the optical Kerr coefficient of the nonlinear rods are 1.4 and 10^{-15} m^2/W, respectively. The radius of these defects is chosen according to the functionality of each resonator. The resonant wavelength of the ring (λ_r) is defined as

$$\lambda_r = \frac{2\pi R n_{\text{eff}}}{m}$$

where R is the radius, n_{eff} is the effective refractive index of the ring, and m is an integer number. According to the optical Kerr effect, the refractive index of the nonlinear rod depends on the amount of the optical intensity. Concerning the working states, different optical intensities reach the rings and change the effective refractive index. As a result, by choosing the proper values for the radius of nonlinear rods, the resonant wavelength

can be tuned for coupling between two waveguides. So, the different switching thresholds can be obtained for different radii of nonlinear rods. The radii of 126, 126, 129, 115, 123, and 132 nm are used to obtain the switching threshold at optical intensities of 8, 8, 6, 16, 10, and 4 W/μm^2 for R1, R2, R3, R4, R5, and R6, respectively. To tune the mentioned values, the radii of nonlinear rods were scanned by a step of 1 nm. Radius of rods at the cross-connection of waveguides is 70 nm.

3. Results and discussions

To simulate the optical waves, the finite-difference time-domain (FDTD) method is used. In this method, components of the electric and magnetic fields for Maxwell's equations should be calculated at the time and space domains. Concerning the used radii in the structure, the length of the unit cell is chosen as 10 nm. According to Courant's condition, the time step of 1 as is used, and the perfectly matched layer (PML) is considered as the boundary condition. The optical waves with a wavelength of 1550 nm are applied to the input ports.

The structure includes X, Y, and Z input ports so for obtaining a full-subtractor in which the operation of X-Y-Z be correctly done, eight possible states should be simulated as follows (as shown in Fig. 2).

State 1: When all input ports are OFF, there is no signal inside the structure so both output ports will be OFF.

State 2: When X is ON and Y and Z are OFF, the amount of optical intensity inside W2 waveguide is around 8 W/μm^2. Therefore, as discussed previously, R1 and R2 drop the optical waves into W3 and W7, respectively. The waves inside W3 reach D port and turn it ON. On the other hand, the optical waves inside W7 travel toward W6 and W8 so the amount of optical intensity inside W8 is lower than the required switching threshold for R6. So, R6 does not drop them into W9 and no optical waves reach B port. As a result, in this state, B will remain OFF (Fig. 2(a)).

States 3 and 4: In these states, X is OFF and only one of Y or Z is ON (X = Z = 0, Y = 1 or X = Y = 0, Z = 1). So, R5 drops the very little portion of optical waves into W6, and the major portion goes toward W2. R1 and R2 drop the optical waves into W3 and W7. The waves inside W3 reach D port and turn it ON. On the other hand, the optical waves inside W7 travel toward W6 and W8. In this state, the amount of optical intensity inside W8 is as high as the required switching threshold for R6. So, R6 drops the optical waves into W9 and guides them toward B through W9 and W10. As a result, B will be ON too (Figs. 2(b) and (c)).

State 5: In this state, X is OFF and other ports are ON. So, R4 drops most of the optical waves from W4 into W5 and guides them toward B through W5 and W10. As a result, B port will be ON. The other portion of the optical waves travels toward W2, but it is less than the switching threshold required for R1, R2, and R3. So, none of them drop the waves and D port will be OFF (Fig. 2(d)).

States 6 and 7: When X is ON, and only one of Y or Z is ON (X = Y = 1, Z = 0 or X = Z = 1, Y = 0) a very small portion of optical waves is dropped by R5 into W6 and

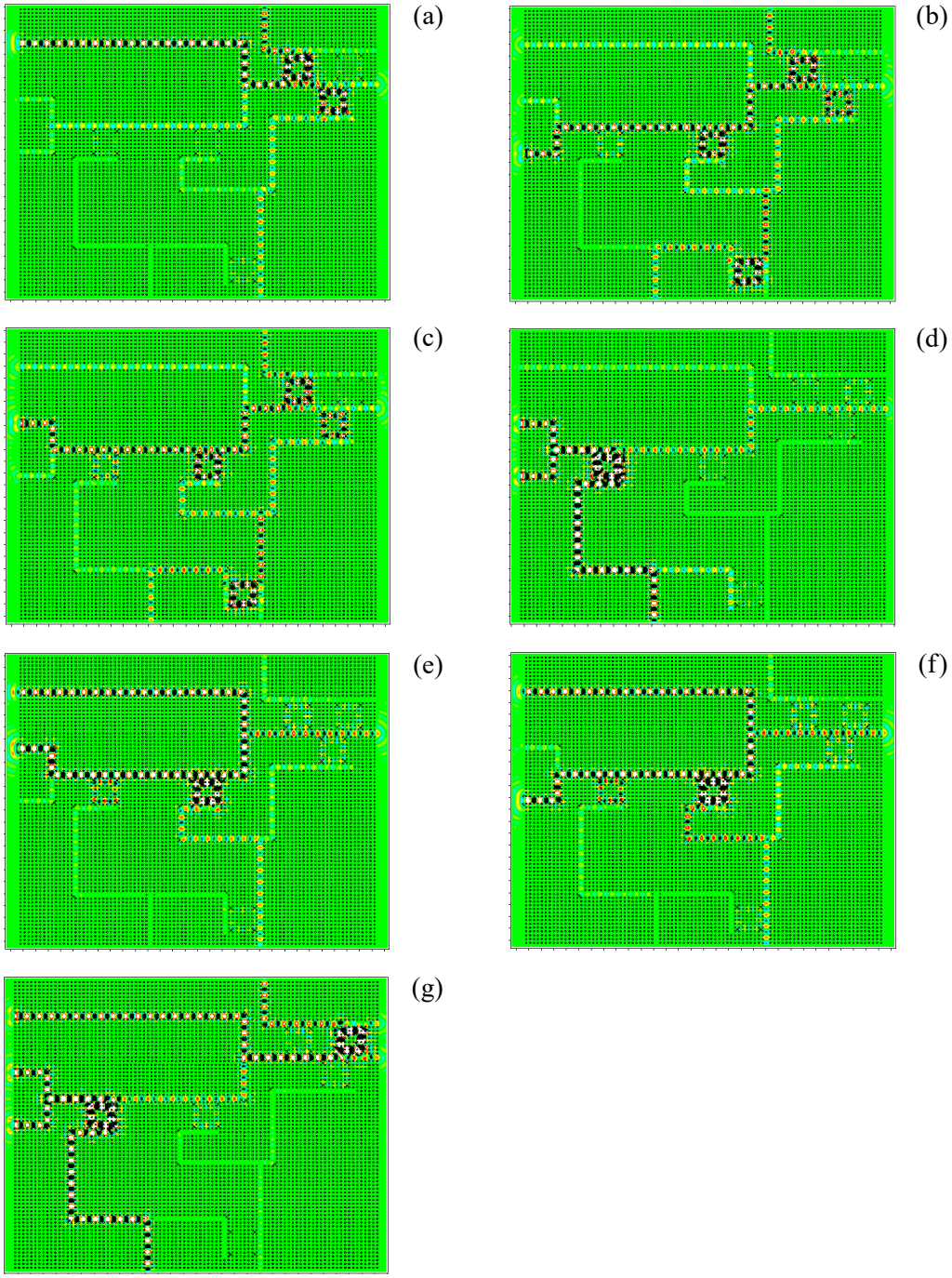

Fig. 2. Optical waves propagation inside the structure for different states: (a) X = 1, Y = Z = 0; (b) X = Y = 0, Z = 1; (c) X = Z = 0, Y = 1; (d) X = 0, Y = Z = 1; (e) X = Y = 1, Z = 0; (f) X = Z = 1, Y = 0; and (g) X = Y = Z = 1.

the rest will go toward W2. Due to destructive interferences, the amount of optical intensity inside W2 is less than 8 W/μm^2, therefore none of the resonators located around W2 drop the optical waves. As a result, D port will be OFF. The amount of optical intensity that reaches W8 through W6 and W7 is very low, therefore R6 does not drop them into W9 and no optical waves reach B. So, in this state B will be OFF too (Figs. 2(e) and (f)).

State 8: When all input ports are ON, R4 drops most of the optical waves from W4 into W5 and guides them toward B through W5 and W10, so B will be ON. The other portion of the optical waves travels toward W2 and joins to the optical waves coming from X. The amount of optical intensity inside W2 reaches the switching threshold required for R3, so it drops the waves into W3 and guide them toward D. In this state, D will be ON too (Fig. 2(g)).

Figure 2 demonstrates the correct operation of the structure and the incoming optical waves are transmitted to the desired output ports through the resonant rings for all possible states. To obtain the time response, the step signals are applied to the input ports for the mentioned states and the normalized power at both output ports is calculated (as shown in Fig. 3). The normalized value is defined as the output power divided by the power at one input port. So, the calculated values may exceed 1.

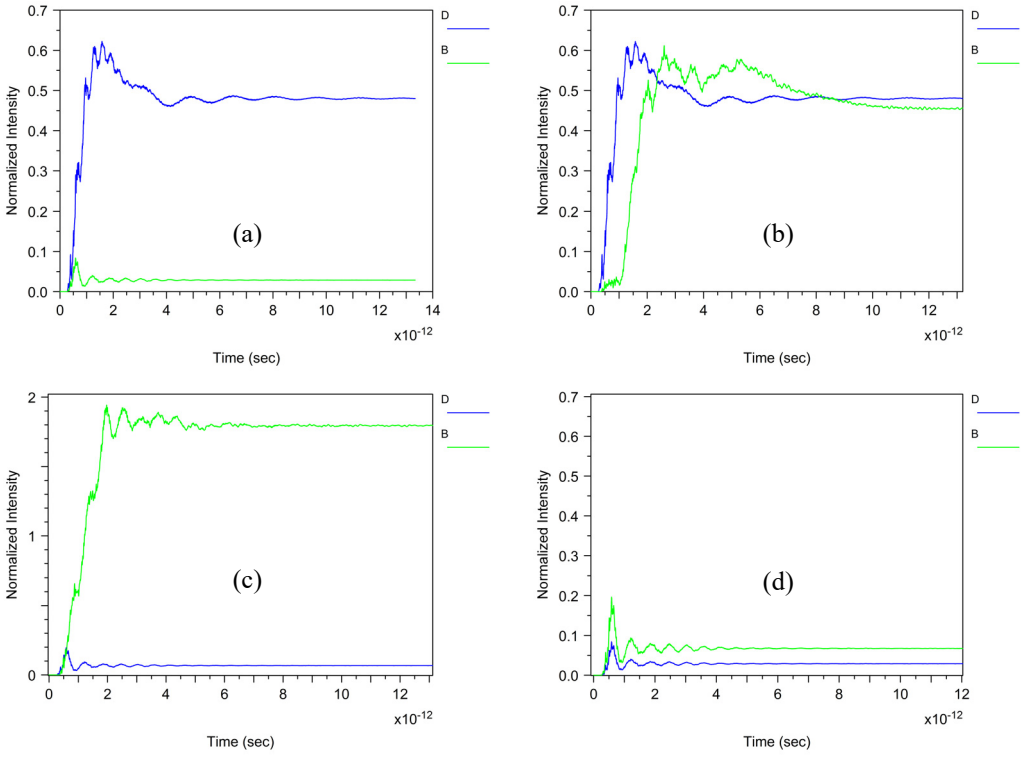

Fig. 3. Time response of the structure for different states: (a) X = 1, Y = Z = 0; (b) X = Y = 0, Z = 1 or X = Z = 0, Y = 1; (c) X = 0, Y = Z = 1; (d) X = Y = 1, Z = 0 or X = Z = 1, Y = 0; and (e) X = Y = Z = 1.

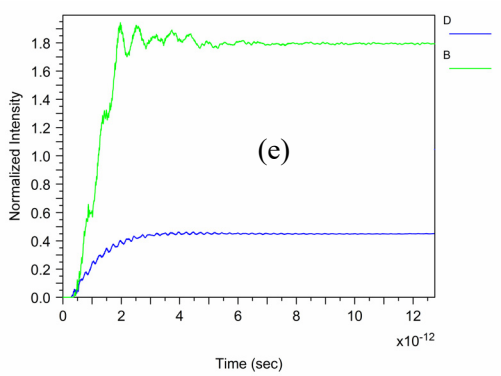

Fig. 3. Continued.

Concerning the simulation results, it can be seen that the maximum rise time of the structure is around 2 ps. This time is defined as the time that a signal reaches a 90% final value. More details of the time analysis have been given in Table 1.

T a b l e 1. Time analysis of the structure.

Input ports			Output ports				Rise time [ps]
			Normalized power [%]		Logic		
X	Y	Z	B	D	B	D	
0	0	0	0	0	0	0	–
0	0	1	45	47	1	1	1.8
0	1	0					
0	1	1	175	5	1	0	1.8
1	0	0	3	48	0	1	1
1	0	1	7	3	0	0	0.5
1	1	0					
1	1	1	180	45	1	1	2

The maximum amount of the normalized powers for logic 0 is assumed as the low margin (M0). Also, the high margin (M1) is considered for the minimum value of them when the output port is at logic 1. According to Table 1, M0 and M1 are equal to 7% and 45% for B port and they are equal to 5% and 47% for D port, respectively. The contrast ratio is defined by $10\log(\mathrm{M1}/\mathrm{M0})$ so this ratio is around 8.08 dB for B port and 9.73 dB for D port. The area of the structure is approximately determined by $N \times L \times a^2$ where N and L are the numbers of rods in horizontal and vertical directions. Concerning $N = 77$, $L = 91$, and $a = 631$ nm, the area is equal to 2790 μm^2. The comparison of the obtained results to other results has been given in Table 2. It can be seen that most of the structures have been designed for the half-subtraction while the full-subtraction is needed for use in optical circuits. The designed structure is faster than Ref. [45] which shows an improvement in presenting the fast full-subtractors. The main advantage of

T a b l e 2. The comparison of the obtained results with other works.

	Rise time [ps]	Subtraction	The smallest radius [nm]	Contrast ratio [dB]	Phase shift/ inequal power
[36]	0.1	Half	57	6.98	Yes
[37]	0.8	Half	36	6.8	No
[38]	3	Half	63	8.31	No
[39]	1	Half	58.5	8	No
[40]	2	Half	110	7.2	Yes
[41]	0.8	Half	36	10.31	No
[42]	1.4	Half	60	9.1	No
[43]	1.5	Half	35	5	Yes
[44]	1.5	Half	–	18.3	–
[45]	2.2	Full	75	9.8	No
This work	2	Full	70	8.08	No

the proposed structure in comparison to another full-subtractor is the fast response time. As far as we know, it is highly needed that the output ports follow the variation of optical power at input ports. This feature makes the correct response of the device for high working frequencies.

Some attempts have been done for the fabrication of the photonic crystal structures using colloidal self-assembly, electron beam lithography, and direct writing via multiphoton microlithography methods [46–55]. A silicon layer is deposited by RF sputter deposition on the top of a glass substrate. Then, using a mask and electron beam lithography, some holes in silicon are created. The holes are filled with the doped-glass. Then, a mask is used to define the patterns for the silicon rods. A mixture of NF_3/CCl_2F_2 at 150 W and 20 mTorr is used to etch the desired section of Si layers. Based on the mentioned reports, radii as small as 70 nm have been fabricated. The minimum value of the radius in the proposed structure is also equal to 70 nm. Therefore, one can be optimistic about the feasibility of fabrication for the presented full-subtractor. The rise time of 2 ps, the area of 2790 μm^2, and the contrast ratio of 8.08 dB promise the designed structure for optical processing applications.

4. Conclusion

An all-optical full-subtractor was designed using 6 nonlinear resonant rings with different switching thresholds. The switching threshold of the resonators was tuned using the radius of nonlinear rods. The simulation results show the proposed structure works as an all-optical full-subtractor. The rise time and the contrast ratio of the proposed device are equal to 2 ps and 8.08 dB, respectively. Also, the area of the structure is around 2790 μm^2. According to the obtained results, it seems that the presented all-optical full -adder is capable to be used in optical processing systems.

References

[1] John S., *Strong localization of photons in certain disordered dielectric superlattices*, Physical Review Letters **58**(23), 1987: 2486–2489, DOI: 10.1103/PhysRevLett.58.2486.

[2] Daghooghi T., Soroosh M., Ansari-Asl K., *A low-power all optical decoder based on photonic crystal nonlinear ring resonators*, Optik **174**, 2018: 400–408, DOI: 10.1016/j.ijleo.2018.08.090.

[3] Tanabe T., Notomi M., Mitsugi S., Shinya A., Kuramochi E., *Fast bistable all-optical switch and memory on a silicon photonic crystal on-chip*, Optics Letters **30**(19), 2005: 2575–2577, DOI: 10.1364/OL.30.002575.

[4] Mehdizadeh F., Soroosh M., *Designing of all optical NOR gate based on photonic crystal*, Indian Journal of Pure and Applied Physics **54**(1), 2016: 35–39.

[5] Miyoshi Y., Ikeda K., Tobioka H., Inoue T., Namiki S., Kitayama K., *Ultra fast all-optical logic gate using a nonlinear optical loop mirror based multi-periodic transfer function*, Optics Express **16**(4), 2008: 2570–2577, DOI: 10.1364/OE.16.002570.

[6] Mohebbi Z., Nozhat N., Emami F., *High contrast all-optical logic gates based on 2D nonlinear photonic crystal*, Optics Communications **355**, 2015: 130–136, DOI: 10.1016/J.OPTCOM.2015.06.023.

[7] Hassangholizadeh-Kashtiban M., Alipour-Banaei H., Tavakoli M. B., Sabbaghi-Nadooshan R., *An ultra fast optical reversible gate based on electromagnetic scattering in nonlinear photonic crystal resonant cavities*, Optical Materials **94**, 2019: 371–377, DOI: 10.1016/j.optmat.2019.06.014.

[8] Jiang Y.-C., Liu S.-B., Zhang H.-F., Kong X.-K., *Reconfigurable design of logic gates based on a two-dimensional photonic crystals waveguide structure*, Optics Communications **332**, 2014: 359–365, DOI: 10.1016/j.optcom.2014.07.038.

[9] Moniem T.A., *All-optical XNOR gate based on 2D photonic-crystal ring resonators*, Quantum Electronics **47**(2), 2017: 169–172, DOI: 10.1070/QEL16279.

[10] Daghooghi T., Soroosh M., Ansari-Asl K., *Ultra-fast all-optical decoder based on nonlinear photonic crystal ring resonators*, Applied Optics **57**(9), 2018: 2250–2257, DOI: 10.1364/AO.57.002250.

[11] Daghooghi T., Soroosh M., Ansari-Asl K., *A novel proposal for all-optical decoder based on photonic crystals*, Photonic Network Communications **35**, 2018: 335–341, DOI: 10.1007/s11107-017-0746-4.

[12] Mehdizadeh F., Alipour-Banaei H., Serajmohammadi S., *Design and simulation of all optical decoder based on nonlinear PhCRRs*, Optik **156**, 2018: 701–706, DOI: 10.1016/j.ijleo.2017.12.011.

[13] Khosravi S., Zavvari M., *Design and analysis of integrated all-optical 2 × 4 decoder based on 2D photonic crystals*, Photonic Network Communications **35**, 2018: 122–128, DOI: 10.1007/s11107-017-0724-x.

[14] Gholamnejad S., Zavvari M., *Design and analysis of all-optical 4--2 binary encoder based on photonic crystal*, Optical and Quantum Electronics **49**, 2017, 302, DOI: 10.1007/s11082-017-1144-y.

[15] Moniem T.A., *All-optical digital 4 × 2 encoder based on 2D photonic crystal ring resonators*, Journal of Modern Optics **63**(8), 2016: 735–741, DOI: 10.1080/09500340.2015.1094580.

[16] Haddadan F., Soroosh M., *Low-power all-optical 8-to-3 encoder using photonic crystal-based waveguides*, Photonic Network Communications **37**, 2019: 83–89, DOI: 10.1007/s11107-018-0795-3.

[17] Salimzadeh A., Alipour-Banaei H., *An all optical 8 to 3 encoder based on photonic crystal OR-gate ring resonators*, Optics Communications **410**, 2018: 793–798, DOI: 10.1016/j.optcom.2017.11.036.

[18] Serajmohammadi S., Alipour-Banaei H., Mehdizadeh F., *Proposal for realizing an all-optical half adder based on photonic crystals*, Applied Optics **57**(7), 2018: 1617–1621, DOI: 10.1364/AO.57.001617.

[19] Rahmani A., Mehdizadeh F., *Application of nonlinear PhCRRs in realizing all optical half-adder*, Optical and Quantum Electronics **50**, 2018, 30, DOI: 10.1007/s11082-017-1301-3.

[20] Cheraghi F., Soroosh M., Akbarizadeh G., *An ultra-compact all optical full adder based on nonlinear photonic crystal resonant cavities*, Superlattices and Microstructures **113**, 2018: 359–365, DOI: 10.1016/j.spmi.2017.11.017.

[21] Neisy M., Soroosh M., Ansari-Asl K., *All optical half adder based on photonic crystal resonant cavities*, Photonic Network Communications **35**, 2018: 245–250, DOI: 10.1007/s11107-017-0736-6.
[22] Andalib A., *A novel proposal for all-optical Galois field adder based on photonic crystals*, Photonic Network Communications **35**, 2018: 392–396, DOI: 10.1007/s11107-017-0756-2.
[23] Jalali P., Andalib A., *Application of nonlinear PhC-based resonant cavities for realizing all optical Galois Filed adder*, Optik **180**, 2019: 498–504, DOI: 10.1016/j.ijleo.2018.11.125.
[24] Jalali-Azizpoor M.R., Soroosh M., Seifi-Kavian Y., *Application of self-collimated beams in realizing all-optical photonic crystal-based half-adder*, Photonic Network Communications **36**, 2018: 344–349, DOI: 10.1007/s11107-018-0786-4.
[25] Serajmohammadi S., Alipour-Banaei H., Mehdizadeh F., *A novel proposal for all optical 1-bit comparator using nonlinear PhCRRs*, Photonics and Nanostructures - Fundamentals and Applications **34**, 2019: 19–23, DOI: 10.1016/j.photonics.2019.01.002.
[26] Surendar A., Asghari M., Mehdizadeh F., *A novel proposal for all-optical 1-bit comparator using nonlinear PhCRRs*, Photonic Network Communications **38**, 2019: 244–249, DOI: 10.1007/s11107-019-00853-z.
[27] Zhu L., Mehdizadeh F., Talebzadeh R., *Application of photonic-crystal-based nonlinear ring resonators for realizing an all-optical comparator*, Applied Optics **58**(30), 2019: 8316–8321, DOI: 10.1364/AO.58.008316.
[28] Mehdizadeh F., Soroosh M., Alipour-Banaei H., Farshidi E., *A novel proposal for all optical analog-to-digital converter based on photonic crystal structures*, IEEE Photonics Journal **9**(2), 2017: 4700311, DOI: 10.1109/JPHOT.2017.2690362.
[29] Mehdizadeh F., Soroosh M., Alipour-Banaei H., Farshidi E., *All optical 2-bit analog to digital converter using photonic crystal based cavities*, Optical and Quantum Electronics **49**, 2017, 38, DOI: 10.1007/s11082-016-0880-8.
[30] Mehdizadeh F., Soroosh M., Alipour-Banaei H., Farshidi E., *Ultra-fast analog-to-digital converter based on a nonlinear triplexer and an optical coder with a photonic crystal structure*, Applied Optics **56**(7), 2017: 1799–1806, DOI: 10.1364/AO.56.001799.
[31] Tavousi A., Mansouri-Birjandi M.A., Saffari M., *Successive approximation-like 4-bit full-optical analog-to-digital converter based on Kerr-like nonlinear photonic crystal ring resonators*, Physica E: Low-dimensional Systems and Nanostructures **83**, 2016: 101–106, DOI: 10.1016/j.physe.2016.04.007.
[32] Tavousi A., Mansouri-Birjandi M.A., *Optical-analog-to-digital conversion based on successive-like approximations in octagonal-shape photonic crystal ring resonators*, Superlattices and Microstructures **114**, 2018: 23–31, DOI: 10.1016/j.spmi.2017.11.021.
[33] Zamanian-Dehkordi S.S., Soroosh M., Akbarizadeh G., *An ultra-fast all-optical RS flip-flop based on nonlinear photonic crystal structures*, Optical Review **25**, 2018: 523–531, DOI: 10.1007/s10043-018-0443-2.
[34] Abbasi A., Noshad M., Ranjbar R., Kheradmand R., *Ultra compact and fast All Optical Flip Flop design in photonic crystal platform*, Optics Communications **285**(24), 2012: 5073–5078, DOI: 10.1016/j.optcom.2012.06.095.
[35] Zhao T., Asghari M., Mehdizadeh F., *An all-optical digital 2-to-1 multiplexer using photonic crystal-based nonlinear ring resonators*, Journal of Electronic Materials **48**, 2019: 2482–2486, DOI: 10.1007/s11664-019-06947-8.
[36] Parandin F., Malmir M.R., Naseri M., *All-optical half-subtractor with low-time delay based on two-dimensional photonic crystals*, Superlattices and Microstructures **109**, 2017: 437–441, DOI: 10.1016/j.spmi.2017.05.030.
[37] Parandin F., Kamarian R., Jomour M., *A novel design of all optical half-subtractor using a square lattice photonic crystals*, Optical and Quantum Electronics **53**, 2021, 114, DOI: 10.1007/s11082-021-02772-8.
[38] Moradi R., *All optical half subtractor using photonic crystal based nonlinear ring resonators*, Optical and Quantum Electronics **51**, 2019, 119, DOI: 10.1007/s11082-019-1831-y.

[39] Askarian A., Akbarizadeh G., Fartash M., *A novel proposal for all optical half-subtractor based on photonic crystals*, Optical and Quantum Electronics **51**, 2019, 264, DOI: 10.1007/s11082-019-1978-6.
[40] Askarian A., Akbarizadeh G., Fartash M., *All-optical half-subtractor based on photonic crystals*, Applied Optics **58**(22), 2019: 5931–5935, DOI: 10.1364/AO.58.005931.
[41] Askarian A., *Design and analysis of all optical half subtractor in 2D photonic crystal platform*, Optik **228**, 2021, 166126, DOI: 10.1016/j.ijleo.2020.166126.
[42] Soroosh M., Mirali A., Farshidi E., *Ultra-fast all-optical half subtractor based on photonic crystal ring resonators*, Journal of Optoelectronical Nanostructures **5**(1), 2020: 83–100.
[43] Namdari N., Talebzadeh R., *Simple and compact optical half-subtractor based on photonic crystal resonant cavities in silicon rods*, Applied Optics **59**(1), 2020: 165–170, DOI: 10.1364/AO.59.000165.
[44] Fang Y., Tang X., *All optical half-adder/subtractor using photonic-crystal-based nonlinear cavities*, Applied Optics **61**(9), 2022: 2306–2312, DOI: 10.1364/AO.451212.
[45] Khajeheian N., Jamali J., Fatehi-Dindarlou M., Taghizadeh M., *An all optical full subtractor based on nonlinear photonic crystals*, Optik **245**, 2021, 167751, DOI: 10.1016/j.ijleo.2021.167751.
[46] Lowell D., Hassan S., Sale O., Adewole M., Hurley N., Philipose U., Chen B., Lin Y., *Holographic fabrication of graded photonic super-quasi-crystals with multiple-level gradients*, Applied Optics **57**(22), 2018: 6598–6604, DOI: 10.1364/AO.57.006598.
[47] Pang L., Nakagawa W., Fainman Y., *Fabrication of two-dimensional photonic crystals with controlled defects by use of multiple exposures and direct write*, Applied Optics **42**(27), 2003: 5450–5456, DOI: 10.1364/AO.42.005450.
[48] Campbell M., Sharp D.N., Harrison M.T., Denning R.G., Turberfield A.J., *Fabrication of photonic crystals for the visible spectrum by holographic lithography*, Nature **404**, 2000: 53–56, DOI: 10.1038/35003523.
[49] Lowell D., Hassan S., Adewole M., Philipose U., Chen B., Lin Y., *Holographic fabrication of graded photonic super-crystals using an integrated spatial light modulator and reflective optical element laser projection system*, Applied Optics **56**(36), 2017: 9888–9891, DOI: 10.1364/AO.56.009888.
[50] Liu Y., Liu S., Zhang X., *Fabrication of three-dimensional photonic crystals with two-beam holographic lithography*, Applied Optics **45**(3), 2006: 480–483, DOI: 10.1364/AO.45.000480.
[51] Ku H.M., Huang C.Y., Chao S., *Fabrication of three-dimensional autocloned photonic crystal on sapphire substrate*, Applied Optics **50**(9), 2011: C1-C4, DOI: 10.1364/AO.50.0000C1.
[52] Schueller O.J.A., Whitesides G.M., Rogers J.A., Meier M., Dodabalapur A., *Fabrication of photonic crystal lasers by nanomolding of solgel glasses*, Applied Optics **38**(27), 1999: 5799–5802, DOI: 10.1364/AO.38.005799.
[53] Chen J.H., Huang Y.T., Yang Y.L., Lu M.F., Shieh J.M., *Design, fabrication, and characterization of Si-based ARROW photonic crystal bend waveguides and power splitters*, Applied Optics **51**(24), 2012: 5876–5884, DOI: 10.1364/AO.51.005876.
[54] Cui L., Zhang Y., Wang J., Ren Y., Song Y., Jiang L., *Ultra-fast fabrication of colloidal photonic crystals by spray coating*, Macromolecular Rapid Communications **30**(8), 2009: 598–603, DOI: 10.1002/marc.200800694.
[55] Von Freymann G., Kitaev V., Lotsch B.V., Ozin G.A., *Bottom-up assembly of photonic crystals*, Chemical Society Reviews **42**(7), 2013: 2528–2554, DOI: 10.1039/c2cs35309a.

Received March 19, 2022
in revised form June 17, 2022